Crystallization Kinetics and Thermal Stability of Ge$_{100-x}$ Sb$_x$ Amorphous Alloys

M. S. Abo-Ghazala[1], N. M. Abdel-Moniem[2], M. Al Buhairi[3] and A. Ali[3]

[1] Physics Department, Faculty of Science, Monoufia University, Shebin EI-Koum, Egypt
[2] Physics Department, Faculty of Science, Tanta University, Tanta, Egypt.
[3] Physics Department, Faculty of Applied Science, Taiz University, Taiz, Yemen.

Abstract: *Amorphous alloys of Ge$_{100-x}$ Sb$_x$ (where x = 5, 50 and 95 at. %) were prepared by the usual melt quench technique. The amorphous nature of the studied compositions was verified via X-ray diffraction. The thermal conductivity of Ge$_{100-x}$Sb$_x$ amorphous alloys were measured versus annealing time at various selected temperatures. The results revealed a slight increase in the thermal conductivity with increasing the annealing time while a decrease in the thermal conductivity is observed with rising the annealing temperature which is attributed to decrease of the heat capacity and the mean free path of the phonons in the alloys. The compositional dependence behavior of the thermal conductivity is explained on the basis of ionicity and free carrier concentration. Results of differential scanning calorimetric (DSC) under non-isothermal are reported and discussed.*

I.   Introduction

Chalcogenide glasses are promising for the application in integrated non-linear optical components due to their high refractive index, large nonlinearities, as well as low optical loss [1]. Crystallization kinetics in the glasses play an important role in determining the stability of amorphous materials as well as understanding the crystallization mechanism [2-4] and directing the subsequent annealing processing of chalcogenide glasses.

The present paper concentrats on the crystallization kinetics and the evaluation of the crystallization parameters for Ge$_{100-x}$ Sb$_x$ (where x = 5, 50 and 95 at. %) bulk alloys by using isothermal method. On the other hand, the study differential scanning calorimetry (DSC) and X-ray diffraction (XRD) is carried out to determine the structural change in these alloys.

II.   Experimental Techniques

2.1. Sample preparation

High purity elements of Ge$_{100-x}$ Sb$_x$ (x= 5, 50 and 95 at. %) were prepared by the melt quenching technique. Cylindrical disks of thickness 2.5 mm and diameter of 13 mm were pressed by die using a pressure machine at a load of 5 tons. Using X-ray diffraction, the bulk samples were found to be in amorphous state.

2.2. Thermal Conductivity Measurements:

Thermal conductivity (λ) at different temperatures was measured using electric circuit and a sample holder. The electrical circuit used for the simultaneous measurements is simply consists of power supply connected in series with a known resistor (heater) generates amount of heat which flows through the sample. An external circuit, which is used to arise the ambient temperature, consists of an electrical oven, voltage transform and temperature controller. The holder of the sample consists of fibrous basis, on which the two concentric cylindrical copper pieces, iron bar and electrical oven are situated. The system was fitted with a heater and sensitive thermocouples for accurate measurements of temperature. The sample was sandwiched between two cylindrical cooper pieces. A pressure contact arrangement was incorporated in the sample holder for better contact between the copper pieces and the sample. A running vacuum of the order of 10^{-3} mbar was maintained in the cell during measurements. The ambient temperature was controlled electronically and measured using digital temperature and controller.

Thermal conductivity was determined by the relation:

$$\lambda = \frac{Q/A}{\Delta T/\Delta L} \dots\dots\dots\dots\dots\dots\dots\dots\dots\dots\dots\dots\dots\dots\dots\dots\dots (1)$$

Where, Q is the amount of heat passing through a cross section, A, and causing a temperature difference, ΔT, over distance of ΔL. Q/A is therefore the heat flux which is causing the thermal gradient, $\Delta T/\Delta L$. The measurement of thermal conductivity, therefore, always involves the measurement of the heat flux and temperature difference. Temperature of both surfaces of the sample was measured with the help of two identical thermocouples. The comparison method for the measurement of the heat flux is used.

Effect of Annealing Time on the Thermal Conductivity

The expression for the lattice thermal conductivity has the form:

$$\lambda_L = \frac{1}{3} CVL \dots\dots\dots\dots\dots\dots\dots\dots\dots\dots\dots\dots\dots\dots\dots\dots\dots\dots\dots\dots (2)$$

Where, C is the heat capacity per unit volume, V is the phonon velocity and L is the phonon mean free path.

2.3. Differential Scanning Calorimetry studies: Differential Scanning Calorimetry (DSC) was carried out on a few mg of the powder samples from the as-prepared specimens using a Perkin-Elmer DSC-2 under pure argon atmosphere. The instrument was calibrated at the temperature corresponding to Ge and Sb melting points and at a constant heating rate. The values of the glass transition temperatures (T_g) and the crystallization temperatures (T_c) were determined using the microprocessor of the thermal analyzer.

2.4. X-ray Diffraction (XRD): X-ray investigation for the bulk specimens was performed utilizing a Philips diffractometer, model (Philips X-ray diffractometer, type Shimadzu XD-3) to examine the amorphous structure of the as-prepared samples. The x-ray patterns were run with Cu target and graphite monochromator. All the diffractograms were carried out at room temperature. The annealed samples at different temperatures are also investigated to show the phases in our alloys. From the X-ray diffraction pattern, the interplaner spacing (d_{hkl}) was calculated according to Bragg's equation:

$$n\gamma = 2d_{hkl}sin\theta \dots\dots\dots\dots\dots\dots\dots\dots\dots\dots\dots\dots (3)$$

Where, γ is the wavelength of the X-ray, θ is the diffraction angle and n is the order of diffraction which is taken as unity.

III.   Results and Discussions

3.1. Time dependence of the thermal conductivity

The behaviors of the thermal conductivity (λ) as a function of the annealing time (t) at different temperatures for the glassy system $Ge_{100-x} Sb_x$, where x = 5, 50 and 95 at. %, respectively are studied perfectly as shown in Figs. 1, 2 and 3.

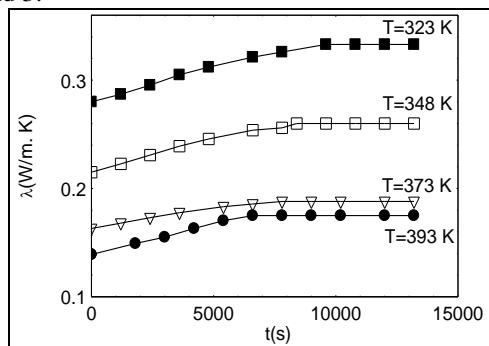**Fig. 1:** Thermal conductivity versus annealing time at Different temperatures for $Ge_{95} Sb_5$ glassy sample.
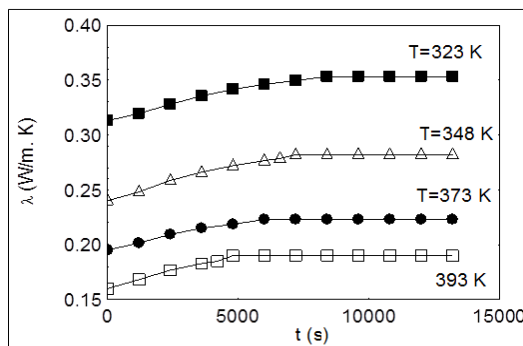

Fig.2: Thermal conductivity versus annealing time at Different temperatures for $Ge_{50}Sb_{50}$ glassy sample.
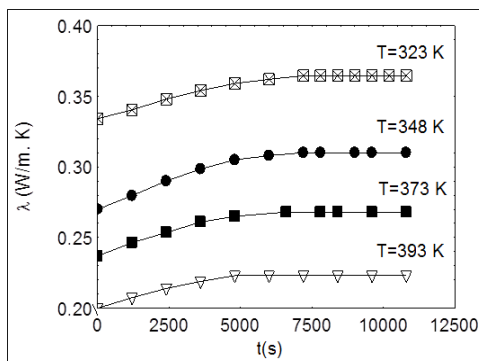

Fig. 3: Thermal conductivity versus annealing time at different temperatures for Ge_5Sb_{95} glassy sample.

It is seen that, the thermal conductivity slightly increases with increasing the annealing time until a certain point, it remains approximately constant for longer annealing times. This slightly increase in the thermal conductivity with annealing time is related to the crystallization of the sample. For similar temperatures, we can see from Figs. 1, 2, and 3 that annealing time required to reach the saturation for $Ge_5 Sb_{95}$ samples is less than that required for $Ge_{50}Sb_{50}$ samples, while samples containing 5% Sb require the longest annealing time to

crystallize, which agree with earlier data indicating that the Ge rich composition caused slow crystallization time [5].

In order Semiconductor, the mean free path is larger than that of disorder material [6]. Therefore, the increase of thermal conductivity of the Ge$_{100-x}$ Sb$_x$ alloys with the annealing time is due to the crystallization effect which leads to the increase of mean free path.

3.2. Kinetics of crystallization using thermal conductivity measurements

The kinetics of crystallization was investigated using the measurements of the thermal conductivity as a function of annealing time. Information on some aspects of the crystallization mechanism was discussed. As crystallization proceeds through nucleation and growth, its kinetics should be described by the Johnson-Mehl-Avrami equation [4]:

$$X = 1 - \exp(-kt^n) \dots\dots\dots\dots\dots\dots\dots\dots\dots\dots \text{(4)}$$

Where,
$$k = k_0 \exp(-E_c/RT) \dots\dots\dots\dots\dots\dots\dots\dots\dots \text{(5)}$$

In eq. (4), X is the volume fraction of the crystalline material transformed from the amorphous state at the time t. In eq. (5), k_0 is a constant, R is the gas constant, E_c is the activation energy for the crystallization process, and n is the Avrami exponent related to the time dependence of nucleation and to the dimensionality of growth. From the results of the thermal conductivity as a function of annealing time, we evaluated the volume fraction of the crystalline material as:

$$X = \frac{\lambda_0 - \lambda_t}{\lambda_0 - \lambda_\infty} \dots\dots\dots\dots\dots\dots\dots\dots\dots\dots\dots \text{(6)}$$

Where, λ_0 is the thermal conductivity at zero time, λ_t is the thermal conductivity at time t and λ_∞ is the thermal conductivity at the full crystallization. According to eq. (4), the value of n can be derived from the slope of the straight line in the plot of ln[-ln(1-X)] versus lnt as shown in Figs. 4, 5 and 6 for the studied Ge$_{100-X}$ Sb$_X$ compositions (where x = 5, 50 and 95 at%), respectively.
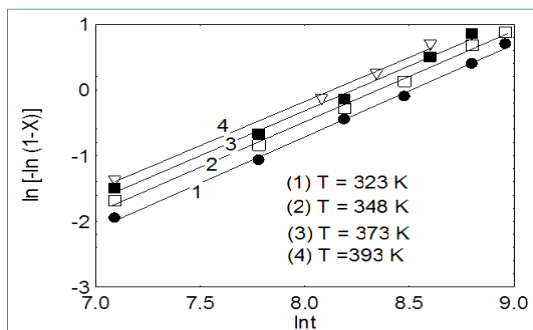

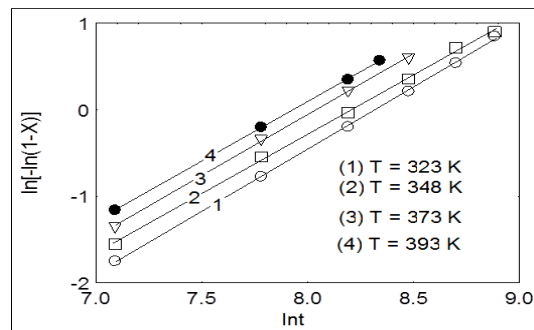**Fig.4**: ln[-ln(1-X)] versus lnt at different temperatures for Ge$_{95}$ Sb$_5$.

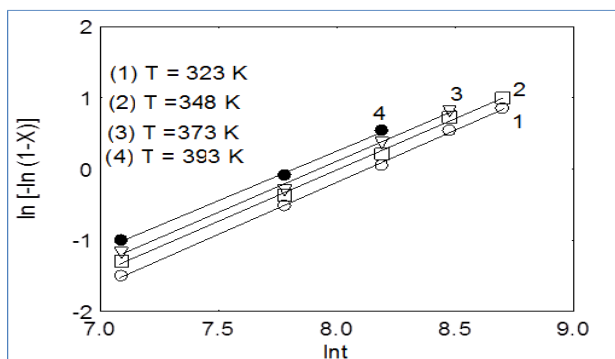**Fig. 5**: ln [-ln(1-X)] versus lnt at different temperatures for Ge$_{50}$ Sb$_{50}$.

Fig. 6: ln [-ln(1-X)] versus lnt at different temperatures for Ge$_5$ Sb$_{95}$.

The values of (n) calculated at 323, 348, 373 and 393 K for the studied compositions are listed in table (1).

Table (1): Date of n at different annealing temperatures for the three Ge$_{100-x}$ Sb$_x$ alloys.

Composition	n			
	T=232K	T=348K	T=373K	T=393K
Ge$_{95}$ Sb$_5$	1.41	1.38	1.37	1.34
Ge$_{50}$ Sb$_{50}$	1.44	1.41	1.41	1.38
Ge$_5$ Sb$_{95}$	1.46	1.44	1.44	1.39

Assuming that the volume fraction of the crystalline material, X, is proportional to the conductivity in the range of crystallinity percolation, we have found that the value of (n) in our samples is close to 1 and does not strongly depend on the composition and annealing temperature.

In Figs. 7, 8 and 9 the values of ln(1-X) as a function of (t^n) for the Ge$_{100-x}$ Sb$_x$ (where x = 5, 50 and 95 at. %) compositions annealed at 323, 348, 373 and 393 K are plotted. From the slopes of this function fitted to the date, we calculated the crystallization reaction rate (k) according to eq. (4) and listed in table (2).
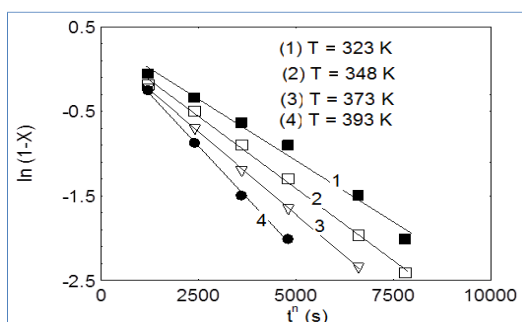
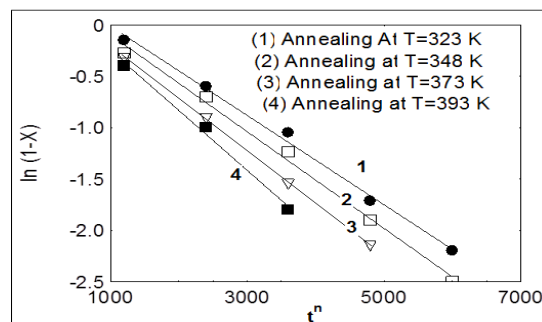**Fig.7**: ln(1-X) versus t^n at different temperatures for Ge$_{95}$Sb$_5$.

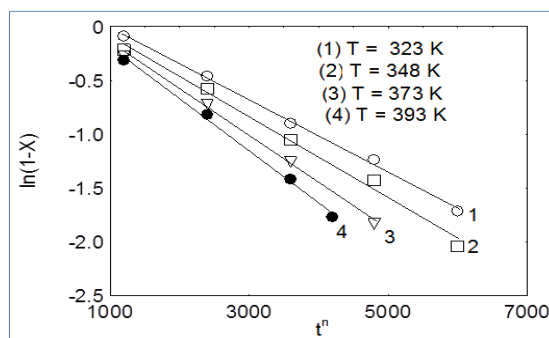**Fig.8**: ln(1-X) versus t^n at different temperatures for Ge$_{50}$ Sb$_{50}$.

Fig. 9: ln(1-X) versus t^n at different temperatures for Ge$_5$ Sb$_{95}$.

Table (2) Values of k at different annealing temperatures for the three Ge$_{100-x}$ Sb$_x$ compositions.

Composition	k			
	T = 323K	T = 348K	T = 373K	T = 393K
Ge$_{95}$ Sb$_5$	0.00208	0.00283	0.00373	0.00456
Ge$_{50}$ Sb$_{50}$	0.00235	0.00304	0.00395	0.00502
Ge$_5$ Sb$_{95}$	0.00271	0.00366	0.00443	0.00584

Plot of ln(k) versus 1000/T for the three Ge$_{100-x}$ Sb$_x$ (where x = 5, 50, and 95 at. %) compositions are shown in Fig. 10.
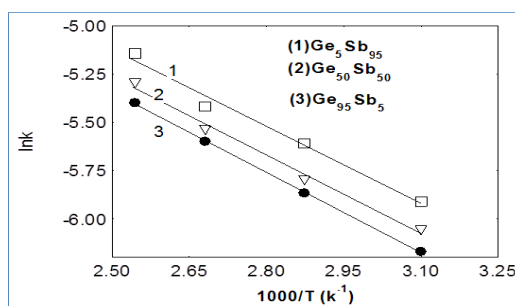
Fig. 10: ln(k) versus 1000/T for Ge$_{100-x}$ Sb$_x$ glassy alloys.

The activation energies for each composition calculated by the slopes of the straight lines according to eq. (5) are listed in table (3).

Table (3): E$_c$ values obtained according to eq. (5) for the three Ge$_{100-x}$ Sb$_x$ samples

| Composition	E$_c$ (kcal/mol)
Ge$_{95}$ Sb$_5$	22.3
Ge$_{50}$ Sb$_{50}$	21.5
Ge$_5$ Sb$_{95}$	20.5

From the results mentioned in table (3), we observed that the activation energy of crystallization decreased with increasing the Sb content, which indicate that the crystallization ability increases with increasing in the Sb content. This fact is confirmed from the rate of crystallization results given in table (2), from which we observe that the rate of crystallization increases with increasing Sb content.

### 3.3. Differential Scanning Calorimetric (DSC) Studies:

This part is concerned with the study of crystallization kinetics and the evaluation of the crystallization parameters for Ge$_{100-x}$ Sb$_x$ (where x = 5, 50 and 95 at %) amorphous alloys by using non-isothermal method. The DSC thermograms were recorded at heating rate of (20 K/min) for the three compositions in the temperature range from 300 K to 800 K. Typical DSC traces are shown in the Figs. 11, 12 and 13 respectively.
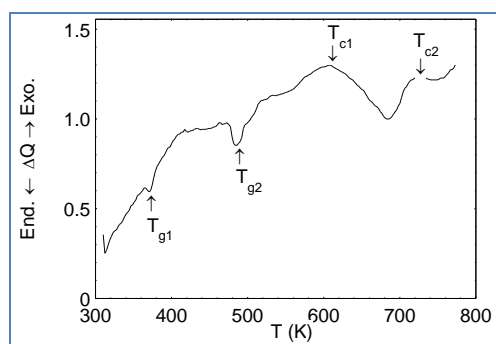
Fig. 11: DSC thermogram of Ge$_{95}$ Sb$_5$ heated at 20 K/min.
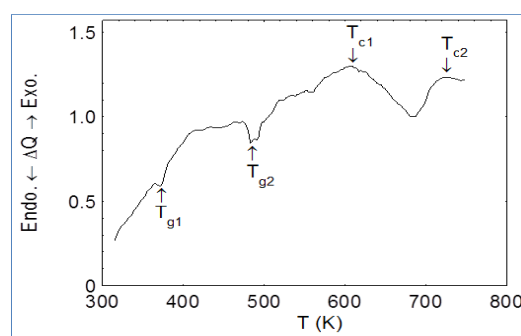
Fig. 12: DSC thermogram of Ge$_{50}$ Sb$_{50}$ heated at 20 K/min.
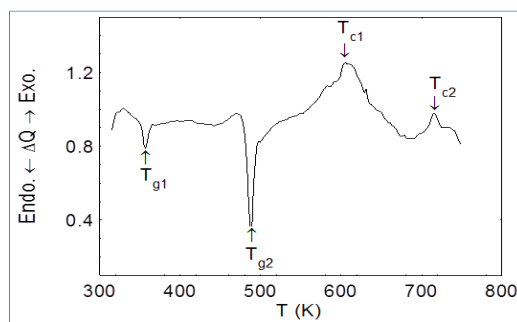
Fig. 13: DSC thermogram of Ge$_5$ Sb$_{95}$ heated at 20 K/min.

It has been reported that, the crystallization temperature T$_C$ is composition dependent and decreasing with Sb content [7]. At high Ge content (x = 95 at %), crystallization leads to two separated phases Ge-Ge and Ge-Sb. At x = 50 at%, Sb crystallize in a first step is followed by Ge crystallization. At x = 95 at%, only Sb crystallizes with [001] zone axis [8].

From Figs. 11, 12 and 13 one can observe that all the samples show two endothermic peaks (T$_{g1}$ and T$_{g2}$) correspond to the glass transition temperatures which is associated with absorbing energy to overcome the rigidity of the lattice. Also, two exothermic peaks shown in the Figs. 11, 12 and 13, were related to the crystallization transition ranges of the crystalline phases. The maxima of the peaks are designated as the crystallization temperatures T$_{c1}$ and T$_{c2}$. Numerical values of these temperatures at heating rate of 20 K/min for Ge$_{95}$ Sb$_5$ are given in Table (4), from which one can observe that all the compositions show that the first crystallization temperature (T$_{c1}$) and the second crystallization temperature (T$_{c2}$) is decreased with increasing Sb content in agreement with [7].

Table (4) Date of T$_g$ and T$_c$ at heating rate of 20 K/min for the three Ge$_{100-x}$ Sb$_x$ compositions.

| Composition	T$_{g1}$ (K)	T$_{g2}$ (K)	T$_{c1}$ (K)	T$_{c2}$ (K)
Ge$_{95}$ Sb$_5$	370	486	608	726
Ge$_{50}$ Sb$_{50}$	371	483	605	721
Ge$_5$ Sb$_{95}$	357	488	603	715

The appearance of a double glass transition indicates unusual phase separation in the glassy alloy. The phase separation leading to double glass transition may arise after the glass to super cooled melt transition or the glass may be diphasic to start with itself. The phenomenon of double glass transition has been observed in many glassy systems [8-12].

On the other hand, the appearance of two crystallization temperature peaks T$_{c1}$ and T$_{c2}$ for this alloy indicates the existence of molecular phase separation which is in agreement with previous results reported for Se-In-Cu [4] and Ge- Se-In [13].

Under nonisothermal conduction, the fraction X crystallized at any temperature T is given as X = (A$_T$/A), where A is the total area of the exotherm between the temperature, T$_i$, where crystallization just begins, and the temperature, T$_f$, where the crystallization is completed, and A$_T$ is the area between T$_i$ and T$_f$. [14, 15]. For nonisothermal crystallization, the volume fraction X of crystals precipitated in a glass heated at a uniform rate is related to E$_C$ through the equation:

$$\ln[-\ln(1-X)] = -n\ln\alpha - 1.052m\,E_C/RT + \text{constant} \quad\text{......(7)}$$

Where, m and n are integer constants depending on the morphology of the growth. The plots between ln[-ln(1-X)] versus 1000/T at heating rate of 20 K/min for the three Ge$_{100-X}$ Sb$_x$ (where, x= 5, 50 and 95 at. %) compositions are shown in the Figs. 14, 15, and 16, respectively.
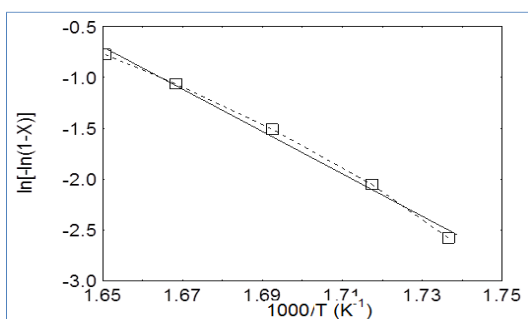
Fig.14: Plot of ln [-ln (1-X)] vs. 1000/T at heating rate of 20K/min for Ge$_{95}$ Sb$_5$ alloy.
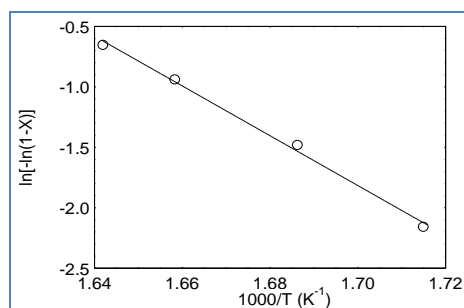
Fig. 15: Plot of ln [-ln(1-X)] vs. 1000/T at heating rate of 20 K/min for Ge$_{50}$ Sb$_{50}$ alloy.
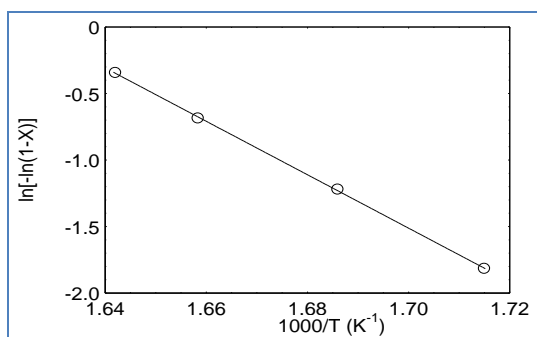
Fig. 16. Plot of ln [-ln(1-X)] vs. 1000/T at heating rate of 20 K/min for Ge$_5$ Sb$_{95}$ alloy.

The values of the activation energies of crystallization (E$_c$) for the three studied compositions obtained from the slopes of the Figs. 14, 15, and 16 according to Eq. (7) are listed in Table (5).

Table (5): E$_c$ values obtained according to eq. (7) for the three Ge$_{100-x}$ Sb$_x$ samples.

Composition	E$_c$ (kcal/mol)
Ge$_{95}$ Sb$_5$	19.748
Ge$_{50}$ Sb$_{50}$	19.462
Ge$_5$ Sb$_{95}$	18.985

From Table (5) we observe that, the activation energy for crystallization is decreased with increasing Sb content, which agrees with results obtained using the measurements of the thermal conductivity as a function of annealing time. These results indicate that the crystallization ability is increase with increasing Sb content.

3.4 X-ray Diffraction Analysis

The X-ray diffractograms of typical virgin Ge$_{100-x}$ Sb$_x$ samples (x= 5, 50 and 95 at%) does not reveal any peak corresponding to Bragg's condition as shown in Fig.17, thus the virgin samples were found to be amorphous.
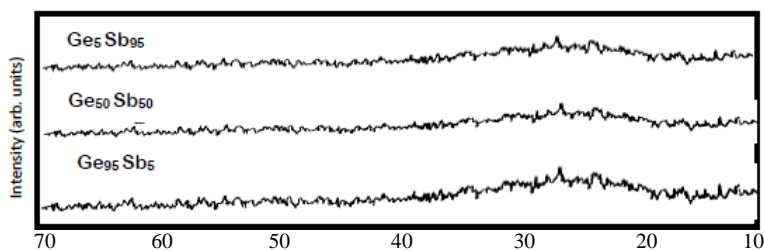

Fig. 17: X-ray diffractogram patterns recorded for as-quenched Ge$_{100-x}$ Sb$_x$ samples.

To show the effect of annealing on the structure of the bulk materials, a-Ge$_{100-x}$ Sb$_x$ (were x = 5, 50 and 95 at. %) bulk samples annealed at 423 K and 593K for different times was investigated by X-ray as shown in Figs 18, 19 and 20, respectively.
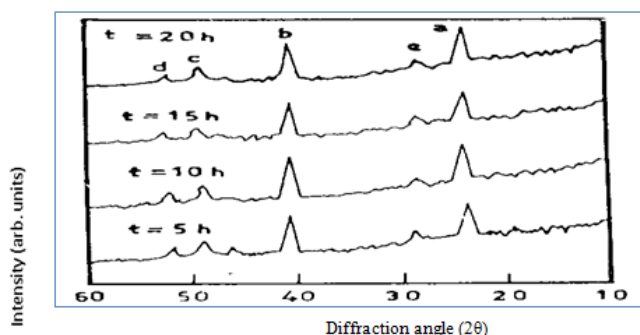

Fig.18: X-ray diffraction records for amorphous Ge$_{95}$ Sb$_5$ bulk sample annealed for different times at 423 K.
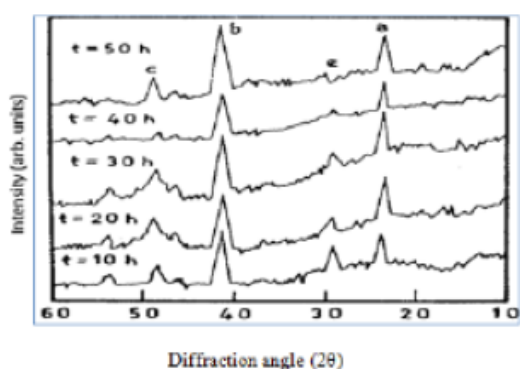

Fig.19: X-ray diffraction records for amorphous Ge$_{50}$ Sb$_{50}$ bulk sample annealed for different times at 593 K.
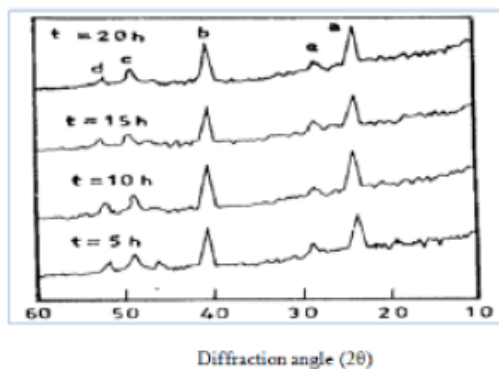
Fig.20: X-ray diffraction records for amorphous Ge$_5$ Sb$_{95}$ bulk sample annealed for different times at 423 K.

The annealing temperatures were selected from DSC thermograms between the glass transition temperature T$_{g2}$ and before the crystallization temperature T$_{c1}$. It is shown that the intensity of each peak appearing in the x-ray pattern is increased with increasing annealing temperature. This means that, the amount of the crystallized formed phases upon annealing increases. The detected peaks reveal that some partial crystallization occurs after annealing. The growth of these peaks with increasing the annealing time shows the growth of the crystalline phase on the expense of the amorphous one. The detected crystalline phases were found to be Ge in the tetragonal form and Sb in the hexagonal form. Also, a new crystalline phase in the hexagonal form was appeared and it may be due to Ge Sb phase as shown in Table 6 for Ge$_{95}$ Sb$_5$. The

crystalline Ge$_{100-x}$ Sb$_x$ phases obtained by annealing showed the presence of Ge crystalline phase in Ge Sb solution [16].

Table. 6: X-ray crystallographic of sample Ge$_{95}$ Sb$_5$ after annealin for different times (h) at 423 K.

Time of annealing t(h)		Experimental			ASTM Cards			
		Crystal Phase	2Θ	d(^{o}A)	Crystal Phase	hkl	d(^{o}A)	Crystal
5	(a)	Unknown	23.8	3.73	--------	--------	--------	----------
	(b)	Sb	40.2	2.24	Sb	2.248	014	Hex.
	(c)	Ge	48.8	1.864	Ge	1.856	301	Tetra.
	(d)	Ge	51.8	1.762	Ge	1.745	004	Tetra.
	(e)	Ge	28.8	3.096	Ge	3.01	012	Tetra.
10	(a)	Unknown	23.7	3.749	--------	--------	--------	----------
	(b)	Sb	40.2	2.24	Sb	2.248	014	Hex.
	(c)	Ge	48.7	1.867	Ge	1.87	310	Tetra.
	(d)	Ge	51.8	1.762	Ge	1.745	004	Tetra.
	(e)	Ge	28.8	3.096	Sb	3.109	102	Hex.
15	(a)	Unknown	23.8	3.749	--------	--------	--------	----------
	(b)	Sb	40.2	2.24	Sb	2.248	014	Hex.
	(c)	---------	48.5	1.867	Ge	1.87	310	Tetra.
					Sb	1.878	006	Hex.
	(d)	Ge	51.8	1.754	Ge	1.745	004	Tetra.
	(e)	Ge	28.8	3.014	Ge	3.01	012	Tetra.
20	(a)	Unknown	23.8	3.749	--------	--------	--------	----------
	(b)	Sb	40.2	2.24	Sb	2.248	014	Hex.
	(c)	---------	48.5	1.867	Ge	1.87	310	Hex.
					Sb	1.878	006	Tetra.
	(d)	Ge	51.8	1.754	Ge	1.745	004	Tetra.
	(e)	Sb	28.8	3.014	Sb	3. 109	102	Hex.

IV. Conclusions

The data of thermal conductivity, λ, of the alloys under study showed that:

i) λ decreases with increasing the temperature, which was attributed to decreasing of the heat capacity and the mean free path.

ii) λ increases with rising the antimony content which was attributed to the increase of the free carrier concentration.

Differential Scanning Calorimetry (DSC) results indicate molecular phase separation by showing double glass transition temperatures and double stage crystallization. The crystallization temperature, T$_c$, and the activation energy of crystallization, E$_c$, were found to be compositional dependent.

Heat treatment of the as-prepared bulk samples induced amorphous-crystalline transformations and the amount of crystalline phases increase with increasing the annealing temperature and annealing time.

References

[1] S. R. Elliot, "physics of Amorphous Materials" New York: John Wiley & Sons, Inc (1990) 35.
[2] J. Singh, "Optoelectronics an Introduction to Materials and Devices", The Mc Grow-Hill companies, New York (1996) 191.
[3] A. B. Magomedov, S. A. Agaev and Kh. O. Alieva, "Thermal Conductivity of Tl Sb Te in solid and molten states", Sov. Phys. Semicond. 21 (3), (1987) 344-345.
[4] M. S. Abo-Ghazala, El-Sayed M. Farag, A. H. Ammar, J. Vac. Sci. Technol. A, Vol. 24, No. 5, Sep/Oct. (2006).
[5] Yong-Goo Yoo, Dong-Seok Yang, Ho-Jun Ryu, Woo Seok Cheong, Man-Cheol Baek, material Science and Engineering, 449, (2007) 627.
[6] J. W. Cristian, in The Theory of Transformations in Metals and Alloys, Pergamon Press, New York, 2nd ed., (1975) 450.
[7] J. M. de Pozo, M. P. Herrero and L. Diaz, J. Non-Cryst. Solids, 185, (1995) 183.
[8] S. Asokan, G. Parthasarathy, J. Non-Cryst. Solids, 86, (1986) 48.
[9] M. A. Abdel-Rahim, A. Y. Abdel-Latief, A. S. Soltan and M. Abu El-Oyoun, Physica B 322 (2002) 252.
[10] G. Parthasarathy, E. S. R. Gopal, J, Mater Sci. Lett., 3, (1984) 754.
[11] Shamshad, A. Khan, M. Zulfequar, M. Husain, Solid State comm., 123, (2002) 463.
[12] M. A. Urena, M. Fontana, B. Aroondo, M. T. Clavaguera-Mora, J. Non-Cryst. Solids 320, (2003) 151.
[13] M. K. Rabical, K. S. Sangunni, and E. S. R. Gopal, J. Non-Cryst. Solids, 188, (1995) 98.
[14] S. Mahdevan, A. Giridhat, and A. K. Singh, J. Non-Cryst. Solids, 88, (1996)
[15] N. Rysava, T. Spasov, and I. Tichy, J. Therm. Anal., 32, (1987) 1015.
[16] El-Sayed M. Farag, optical & Laser Technology, 38, (2006) 14.